

4-2012

Graphene-Based Frequency Tripler

Hong-Yan Chen

Purdue University, chen200@purdue.edu

Joerg Appenzeller

Birck Nanotechnology Center, Purdue University, appenzeller@purdue.edu

Follow this and additional works at: <http://docs.lib.purdue.edu/nanopub>



Part of the [Nanoscience and Nanotechnology Commons](#)

Chen, Hong-Yan and Appenzeller, Joerg, "Graphene-Based Frequency Tripler" (2012). *Birck and NCN Publications*. Paper 1220.
<http://docs.lib.purdue.edu/nanopub/1220>

This document has been made available through Purdue e-Pubs, a service of the Purdue University Libraries. Please contact epubs@purdue.edu for additional information.

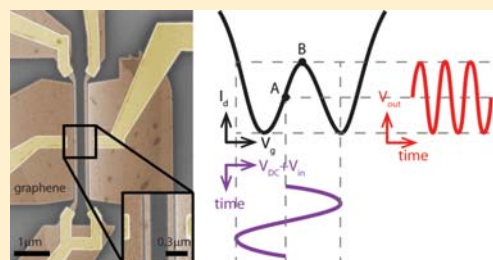
Graphene-Based Frequency Tripler

Hong-Yan Chen* and Joerg Appenzeller*

School of Electrical and Computer Engineering and Birck Nanotechnology Center, Purdue University, West Lafayette, Indiana 47907, United States

ABSTRACT: Graphene has captured the imagination of researchers worldwide as an ideal two-dimensional material with exceptional electrical transport properties. The high electron and hole mobility quickly inspired scientists to search for electronic applications that require high-performance channel materials. However, the absence of a bandgap in graphene immediately revealed itself in terms of ambipolar device characteristics and the nonexistence of a device off-state. The question is: How can the superior electronic properties of graphene be harvested while dealing appropriately with its unique characteristics rather than enforcing conventional device concepts? Here, we report a novel device idea, a graphene-based frequency tripler, an application that employs an innovative electrostatic doping approach and exploits the unique ambipolar behavior of graphene.

KEYWORDS: Frequency multiplier, tripler, spectral purity, ambipolar, electrostatic doping



Frequency multiplication is one of the common approaches for signal generation required in various applications, including digital/analog communication, terahertz radio astronomy, and remote sensing.^{1–3} Conventionally, frequency multiplication is realized by modulating a sinusoidal signal generated at a lower frequency with a nonlinear electronic element (usually a diode or a conventional FET) to generate harmonics at higher frequencies, and the harmonic component of interest is then extracted employing various filter designs. Ideally, frequency multipliers built for all multiplication factors are desirable. However, while it is relatively straightforward to realize a frequency “doubler” by utilizing the nonlinear I – V properties of a diode, a technique widely used in RF/wireless systems, it becomes much more demanding to build a frequency “tripler”. The underlying reason is that the modulated output signal (Figure 1a) of a conventional tripler tends to be dominated by the fundamental frequency component with relatively small power at the third harmonic

frequency. The resulting poor output spectral purity (generally <15%) of the third harmonic component in turn limits the conversion efficiency⁴ and makes complicated filter designs a requirement.^{5–11} Recently, an important breakthrough has been reported that showed improved output spectral purities in frequency doublers based on ambipolar materials.^{12–15} Encouraged by this initial success, we have developed and experimentally demonstrated in this article a novel device concept, a graphene frequency tripler that makes explicit use of graphene’s unique switching properties.

The operation principle of our graphene frequency tripler is illustrated in Figure 2. Two graphene FETs with properly adjusted threshold voltage separation are connected in series. Through the superposition of two V-shaped graphene transfer characteristics, a “W”-shaped current versus gate voltage dependence is obtained as depicted in Figure 2a. This W-shaped characteristic is at the heart of our new device idea since it enables the nonlinear modulation required for creating an output signal with a high spectral purity of the third harmonic as depicted in Figure 2b. The corresponding circuit implementation is shown in Figure 2c. An ac sinusoidal input signal (purple) carrying the fundamental frequency is biased at point A by a dc voltage (V_{DC}) and supplied to the gates of both graphene FETs simultaneously. The amplitude of the input signal is adjusted to create a voltage swing as indicated in Figure 2b by the dashed lines. While the input voltage oscillation follows the cycle from point 1 to 5, the current according to the transfer curve varies and generates an oscillating output voltage through a load resistor (R_L). The resulting output waveform (red), following the corresponding cycle 1 through 5, is

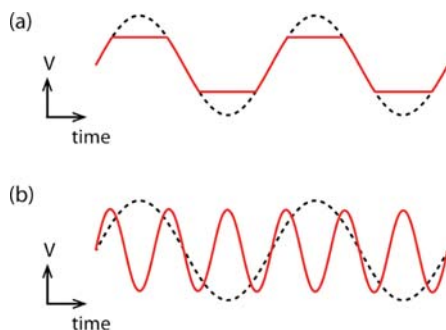


Figure 1. The typical output waveform (solid line) based on a sinusoidal input signal (dashed line) for (a) a conventional frequency tripler and (b) the proposed graphene frequency tripler.

Received: January 18, 2012
Revised: March 1, 2012
Published: March 27, 2012

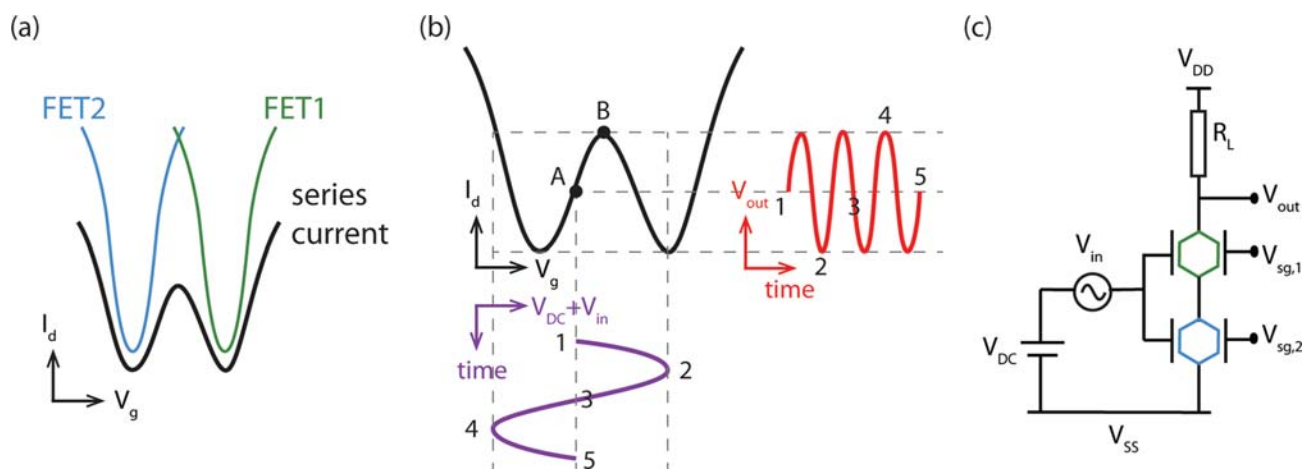


Figure 2. (a) Sketch of the "W"-shaped dc transfer characteristics obtained through connecting FETs with properly adjusted threshold voltage in series. (b) Schematic diagram illustrating the operation principle of a graphene frequency tripler. The input waveform and output waveform are shown in purple and red respectively. The input dc voltage bias (point A) is chosen halfway between the voltages where minimum current occurs and the central current peak (point B). Points in time 1 through 5 in the input cycle correspond to those labeled in the output waveform. (c) Circuit schematic used to implement the graphene frequency tripler. V_{sg1} and V_{sg2} are dc voltages used to control the threshold voltage separation electrostatically between two graphene FETs.

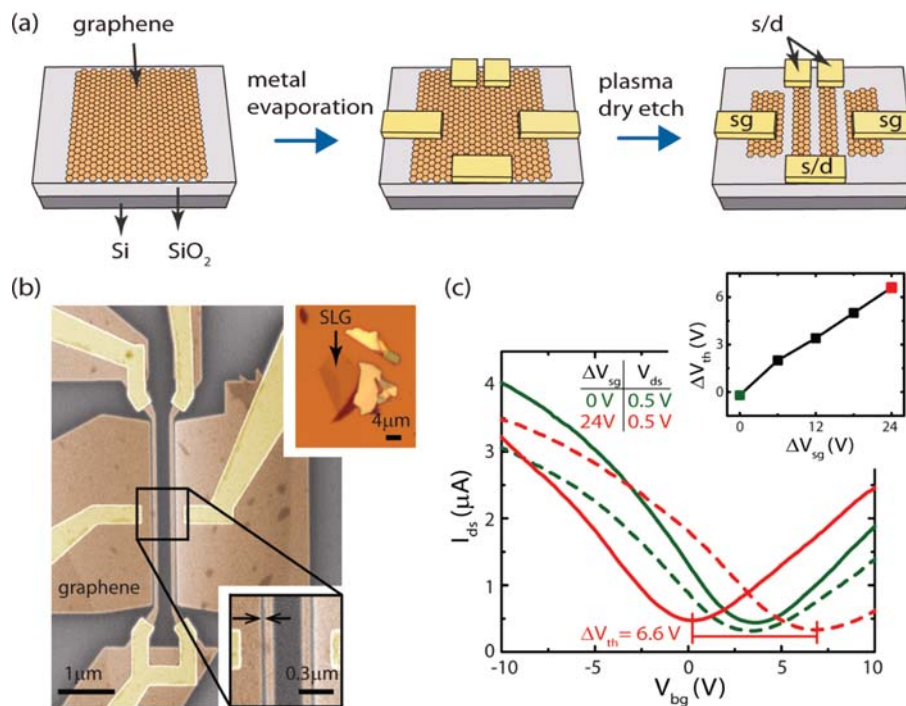


Figure 3. The prototype device structure of our graphene-based tripler. (a) Schematic of the process flow for device fabrication. Graphene flakes are mechanically exfoliated, followed by standard electron-beam lithography for metal evaporation and dry etching (s/d, source/drain; sg, side gate). (b) Optical image (upper right) of an exfoliated graphene flake. The false colored scanning electron micrograph (SEM) image shows the fabricated device on the single-layer graphene (SLG) portion of the flake with the zoom-in SEM image illustrating a clear separation (40 nm) between the side gates and the adjacent channels. (c) Transfer characteristics measured at $\Delta V_{sg} = 0$ V (green) and 24 V (red). Solid line and dashed line represent the two graphene channels. The inset illustrates that ΔV_{th} is approximately a linear function of ΔV_{sg} .

distorted from the input waveform such that the third harmonic is generated as the main component in the output spectrum. Note that by appropriately adjusting the input voltage and amplitude, our approach also allows operating the device as a frequency quadrupler when biasing at point B.

The threshold voltage control in graphene FETs is an indispensable ingredient to enable the operation principle of our graphene frequency tripler. Recently various methods have

been reported on the doping of graphene.^{16–21} Among them, electrostatic doping is advantageous in terms of preserving graphene's electrical properties as well as providing a relatively wide and controllable doping range; both are essential aspects to achieve the W-shaped transfer characteristics shown in Figure 2a. Figure 3 shows our prototype graphene frequency tripler device where electrostatic doping is realized through a side gate structure. The side gates consist of graphene that has

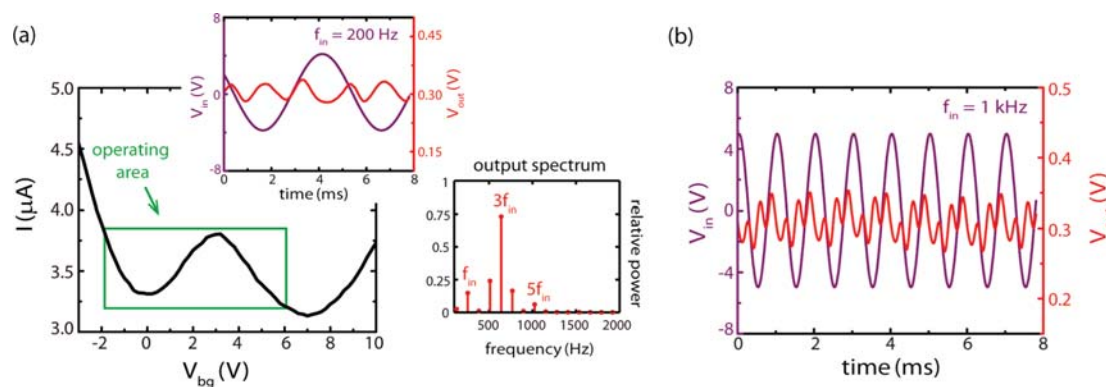


Figure 4. Room-temperature characterization of the fabricated graphene frequency tripler. (a) The “W”-shape of the dc current versus back gate voltage is obtained at $\Delta V_{sg} = 25$ V, $V_{DD} - V_{SS} = 4$ V, $R_L = 98$ k Ω . The inset shows the actual ac input signal of 200 Hz and the measured output waveforms in the time domain. $V_{DC} = 2.2$ V was used to account for the slight asymmetry between the two FETs. The output spectrum in the frequency domain is obtained through Fourier transforming the output waveform at 200 Hz input frequency. (b) Input and output waveforms at an input frequency of 1 kHz. The ac input amplitude is increased to 5 V at this elevated frequency for improved characteristics.

been properly patterned to achieve a small side-gate-to-channel spacing and contacted by metal fingers. The channels of the two serially connected graphene FETs are narrow in width to ensure proper side gate control and relatively long in length to ensure that the supply voltages (V_{DD} , V_{SS}) are in balance with the input voltage applied through the 90 nm back gate. Figure 3c shows the transfer characteristics of the graphene FETs at two side gate voltages (ΔV_{sg}). As apparent from the inset of Figure 3c, the threshold voltage separation between two graphene FETs (ΔV_{th}) increases approximately linearly with ΔV_{sg} .

Figure 4 shows the measured dc transfer current as well as the ac output waveform for one of our graphene-based frequency triplers. The threshold voltage separation of the two graphene FETs was optimized through adjusting ΔV_{sg} to create a W-shaped current versus gate voltage response with the highest possible degree of symmetry. An ac input signal with an amplitude of 4 V is superimposed on a dc bias of 2.2 V and connected to the back gate. Measurements at an input frequency of 200 Hz are performed for proof-of-concept of the desired tripler operation. The resulting output waveform (inset of Figure 4a) shows clear modulation through the W-shaped I – V . The relative output spectrum is obtained by analyzing the Fourier transform of the output waveform. It shows that the spectrum mainly composes of odd harmonics with the third harmonic at 600 Hz dominating the output signal. The fundamental frequency component is substantially suppressed compared with the third harmonic, and higher order harmonic components play a minor role. From these data, we determined that more than 70% of the output power is concentrated at the desired 600 Hz. This corresponds to an improvement of the spectral purity by a factor of almost five compared to conventional triplers (<15%). Moreover, our experimental demonstration shows for the first time that the third harmonic can be generated as the leading component in the output spectrum based on a compact two-FET configuration prior to any filtering. To further characterize the performance of our graphene-based frequency tripler, we also measured the device response at a higher input frequency of 1 kHz (Figure 4b). However, in our prototype devices, the high resistance of the ribbonlike channel ($\sim M\Omega$) and the large parasitic capacitance between the back gate and electrode pads correspond to a cutoff frequency of around 1 kHz, which

currently limits the maximum achievable frequency in our nonoptimized prototype devices. Some distortion in the output waveform becomes visible for a 1 kHz input signal presumably due to the parasitics in our sample layout, resulting in a lower spectral purity compared to the result obtained at an input frequency of 200 Hz.

The output spectral purity in our prototype devices is expected to be enhanced further by improving the symmetry of the W-shaped transfer characteristics. The limited bandwidth is a result of the currently rather large RC time delay, which can be improved by increasing the transconductance through oxide scaling particularly in combination with a top-gated device structure. In principle, graphene frequency triplers operating at radio frequencies are possible considering graphene’s intrinsic high carrier mobility.^{13,22–24}

In conclusion, we have proposed a new device idea that utilizes graphene’s ambipolar device properties to construct a frequency tripler in a compact two-FET configuration and have experimentally verified the operation principle through an electrostatic doping approach. The experimentally achieved spectral purity at an output frequency of 600 Hz is >70%, compared with <15% as generally obtained in conventional FET triplers, which is a significant improvement over existing technologies. Although the bandwidth of our device is currently rather limited, our prototype results on the high spectral purity provide further evidence for graphene as an attractive candidate for future analog applications.

AUTHOR INFORMATION

Corresponding Author

*E-mail: (H.-Y.C.) chen200@purdue.edu; (J.A.) appenzeller@purdue.edu.

Notes

The authors declare no competing financial interest.

ACKNOWLEDGMENTS

H.C. thanks Dr. Wu-Hsin Chen and Saptrashi Das for insightful discussions and Dave Lubelski and Sahil Bansal for assistance with the device fabrication.

REFERENCES

- (1) Raisanen, A. *Proc. IEEE* **1992**, *80*, 1842–1852.

- (2) Faber, M. T.; Chramiec, J.; Adamski, M. E. *Microwave and millimeter-wave diode frequency multipliers*; Artech House: Norwood, MA, 1995.
- (3) Maestrini, A.; Ward, J.; Chattopadhyay, G.; Schlecht, E.; Mehdi, I. *Frequenz* **2008**, *62*, 118–122.
- (4) Output power at third harmonic frequency per input power.
- (5) Ward, J.; Schlecht, E.; Chattopadhyay, G. *IEEE MTT-S International Microwave Symposium, June 6–11, 2004*, Fort Worth, TX, 2004, DOI: 10.1109/MWSYM.2004.1338884.
- (6) Maestrini, A.; Ward, J. S.; Gill, J. J.; Javadi, H. S.; Schlecht, E.; Tripon-Canseliet, C.; Chattopadhyay, G.; Mehdi, I. *IEEE Trans. Microwave Theory Tech.* **2005**, *53*, 2835–2843.
- (7) Maestrini, a.; Ward, J. S.; Tripon-Canseliet, C.; Gill, J. J.; Javadi, H.; Chattopadhyay, G.; Mehdi, I. *IEEE Microwave and Wireless Components Letters* **2008**, *18*, 218–220.
- (8) Campos-Roca, Y.; Verweyen, L.; Fernandez-Barciela, M.; Sanchez, E.; Curras-Francos, M. C.; Bronner, W.; Hulsman, a.; Schlechtweg, M. *IEEE Microwave and Guided Wave Letters* **2000**, *10*, 242–244.
- (9) Fudem, H.; Niehenke, E. C. In *IEEE MTT-S International Microwave Symposium, June 7–12, 1998*, Baltimore, MD, 1998; Vol. 2, pp 387–390, DOI: 10.1109/MWSYM.1998.705015.
- (10) Chiu, J. C.; Chang, C. P.; Houn, M. P.; Wang, Y. H. *IEEE Microwave Wireless Compon. Lett.* **2006**, *16*, 19–21.
- (11) Boudiaf, A.; Bachelet, D.; Rumelhard, C. *IEEE Transactions on Microwave Theory and Techniques* **2000**, *48*, 2546–2553.
- (12) Wang, H.; Nezich, D.; Palacios, T. *IEEE Electron Device Lett.* **2009**, *30*, 547–549.
- (13) Wang, H.; Hsu, A.; Palacios, T. *International Electron Devices Meeting (IEDM)* **2010**, 23.6.1–23.6.4.
- (14) Wang, Z.; Zhang, Z.; Xu, H.; Ding, L.; Wang, S.; Peng, L.-M. *Appl. Phys. Lett.* **2010**, *96*, 173104.
- (15) Wang, Z.; Ding, L.; Pei, T.; Zhang, Z.; Wang, S.; Yu, T.; Ye, X.; Peng, F.; Li, Y.; Peng, L.-M. *Nano Lett.* **2010**, *10*, 3648–55.
- (16) Wang, H.; Wang, Q.; Cheng, Y.; Li, K.; Yao, Y.; Zhang, Q.; Dong, C.; Wang, P.; Schwingenschlögl, U.; Yang, W.; Zhang, X. X. *Nano Lett.* **2012**, *12* (1), 141–144.
- (17) Liu, H.; Liu, Y.; Zhu, D. *Journal of Materials Chemistry* **2011**, *21*, 3335.
- (18) Guo, B.; Fang, L.; Zhang, B.; Gong, J. R. *Insciences J.* **2011**, *1*, 80–89.
- (19) Ishikawa, R.; Bando, M.; Morimoto, Y.; Sandhu, A. *Nanoscale Res. Lett.* **2011**, *6*, 111.
- (20) Giovannetti, G.; Khomyakov, P.; Brocks, G.; Karpan, V.; Brink, J.; van den; Kelly, P. *Phys. Rev. Lett.* **2008**, *101*, 4–7.
- (21) Chen, H. Y.; Appenzeller, J. *Dev. Res. Conf. (DRC)* **2011**, 33–34.
- (22) Lin, Y.-M.; Dimitrakopoulos, C.; Jenkins, K. a; Farmer, D. B.; Chiu, H.-Y.; Grill, A.; Avouris, P. *Science (New York, N.Y.)* **2010**, *327*, 662.
- (23) Liao, L.; Lin, Y.-C.; Bao, M.; Cheng, R.; Bai, J.; Liu, Y.; Qu, Y.; Wang, K. L.; Huang, Y.; Duan, X. *Nature* **2010**, *467*, 305–8.
- (24) Wang, H.; Taychatanapat, T.; Hsu, A.; Watanabe, K.; Taniguchi, T.; Jarillo-Herrero, P.; Palacios, T. *IEEE Electron Device Lett.* **2011**, *32*, 1209–1211.